Available online at www.sciencedirect.com

ScienceDirect

Advances in Climate Change Research xxx (xxxx) xxx

www.keaipublishing.com/en/journals/accr/

Effects of Northern Hemisphere Annular Mode on terrestrial near-surface wind speed over eastern China from 1979 to 2017

Jin-Lin ZHA[a,b], Cheng SHEN[c], Jian WU[a], De-Ming ZHAO[b], Wen-Xuan FAN[a,*], Hui-Ping JIANG[d,e], Cesar AZORIN-MOLINA[f], Deliang CHEN[c]

[a] *Key Laboratory of Atmospheric Environment and Processes in the Boundary Layer Over the Low-Latitude Plateau Region, Department of Atmospheric Science, Yunnan University, Kunming 650091, China*

[b] *Key Laboratory of Regional Climate and Environment for Temperate East Asia, Institute of Atmospheric Physics, Chinese Academy of Sciences, Beijing 100029, China*

[c] *Regional Climate Group, Department of Earth Sciences, University of Gothenburg, Gothenburg 004631, Sweden*

[d] *International Research Center of Big Data for Sustainable Development Goals (CBAS), Beijing 100094, China*

[e] *Key Laboratory of Digital Earth Science, Aerospace Information Research Institute (AIR), Chinese Academy of Sciences, Beijing 100094, China*

[f] *Centro de Investigaciones Sobre Desertificación, Consejo Superior de Investigaciones Científicas (CIDE-CSIC), Moncada Valencia 46008, Spain*

Received 19 March 2022; revised 15 May 2022; accepted 28 October 2022

Abstract

Large-scale ocean−atmosphere circulations (LOACs) have a pronounced effect on the near-surface wind speed (NSWS). In this study, we discussed the contributions of zonal and meridional flows to NSWS changes and identify the possible association between the Northern Hemisphere Annular Mode (NAM) and the NSWS changes over eastern China from 1979 to 2017. Results show that the reduction in NSWS over eastern China was mainly dominated by the weakening of the zonal wind component. NAM has a considerable effect on the NSWS over eastern China. When the NAM exhibits positive phases, the zonal-mean westerly weakens at low-to-mid-latitudes (10°−40°N). Meanwhile, descending flows prevail near 40°N, and ascending flows persist near 65°N in the troposphere. In the lower troposphere, there are northerly anomalies at low-to-mid-latitudes and southerly anomalies at mid-to-high latitudes (40°−70°N). The anomalous meridional flows transport heat from low to high latitudes and weaken the north−south air temperature gradient. The decreased air temperature gradient over East Asia reduces the pressure gradient near the surface, decreasing NSWS in eastern China. NAM variations could dominate (32.0 ± 15.8)% of the changes in the annual mean NSWS. Nevertheless, the contribution of NAM to the interannual changes of the zonal component in NSWS could reach (45.0 ± 12.9)%.

Keywords: Near-surface wind speed; Temperature gradient; Pressure gradient; Northern Hemisphere Annular Mode; Large-scale ocean−atmosphere circulations

1. Introduction

Near-surface wind speed (NSWS) partially governs the energy, water, and momentum transfer between the land surface and lower atmosphere (Kim and Paik, 2015), which affects wind energy production (Pryor and Barthelmie, 2011; Tobin et al., 2016; Wu et al., 2021), evapotranspiration (McVicar et al., 2012), aerosol dispersion (Shi et al., 2019; Zhang et al., 2019a), and air quality (McVicar et al., 2007), among many others. Consequently, an investigation of the long-term changes in NSWS and its causes would be helpful to identify the effects of these processes.

A long-term decrease in NSWS over the global land surface has been confirmed (Vautard et al., 2010). On the regional scale, the NSWS exhibited decreasing trends of −0.09, −0.16,

Abbreviations: NSWS, near-surface wind speed; LOACs, large-scale ocean-atmosphere circulations; NAM, northern hemisphere annular mode.

* Corresponding author.

E-mail address: fanwenxuan@ynu.edu.cn (FAN W.-X.).

Peer review under responsibility of National Climate Center (China Meteorological Administration).

https://doi.org/10.1016/j.accre.2022.10.005

Please cite this article as: ZHA, J.-L et al., Effects of Northern Hemisphere Annular Mode on terrestrial near-surface wind speed over eastern China from 1979 to 2017, Advances in Climate Change Research, https://doi.org/10.1016/j.accre.2022.10.005

−0.12, and −0.07 m s^{-1} per decade in Europe, Central Asia, East Asia, and North America, respectively (Vautard et al., 2010). In Europe, the NSWS reduction was discovered mainly in Turkey (Dadaser-Celik and Cengiz, 2014), Portugal and Spain (Azorin-Molina et al., 2014), and Finland (Laapas and Venalainen, 2018). In Asia, it was reported principally in South Korea (Kim and Paik, 2015) and China (Wu et al., 2016, 2018a; Zha et al., 2017a, 2017b; Zhang et al., 2019b). In North America, the NSWS decrease was found in Canada (Wan et al., 2010) and America (Malloy et al., 2015). Overall, decreased NSWS is a global fact (Wu et al., 2018b). Roderick et al. (2007) termed this decreasing trend in NSWS 'stilling.' In addition to the stilling, a weak increase in the NSWS has also been observed after 2010 (Zha et al., 2021a). Zeng et al. (2019) used the term 'reversal' to describe it. In China, the reversal of stilling has been reported (Li et al., 2018, 2021; Zhang and Wang, 2020), while some researchers emphasized that the turning point of terrestrial stilling is not consistent among different regions (Yang et al., 2012; Li et al., 2018; Zha et al., 2019a, 2021b).

The NSWS decrease can be attributed to external forcing and internal variability (Zhao et al., 2020, 2021; Zha et al., 2021c). The main form of internal variability influencing NSWS is the variation in the large-scale ocean−atmosphere circulations (LOACs). Significant reductions in NSWSs have been observed at a global scale, indicating that the LOACs plays a role in NSWS changes (Earl et al., 2013; Jerez et al., 2013). In China, several studies pointed out that the decreased NSWS was affected by LOACs, e.g., East Asia monsoons (Xu et al., 2006), inter-decadal Pacific Oscillation (IPO) (Fu et al., 2011), and Northern Hemisphere Annular Mode (NAM), also known as Arctic Oscillation (AO) (You et al., 2010; Chen et al., 2013; Lin et al., 2013). The variations in LOACs can induce changes in the temperature and pressure gradients (Wu et al., 2017, 2018b; Li et al., 2018). Therefore, several researchers discussed the relationships between temperature (pressure) gradient and NSWS and proposed that the NSWS changes over China might be primarily due to changes in the pressure-gradient force (Guo et al., 2011; Wu et al., 2018a). Lin et al. (2013) proposed that the spatial gradients of warming or cooling might alter the NSWS at a regional scale through atmospheric thermal adaption. Guo et al. (2017) indicated that the NSWS and air temperature showed negative correlations over and around the Tibetan Plateau, and the most likely cause of the decreased NSWS over the Tibetan Plateau was the asymmetric reduction of the latitudinal surface air temperature gradient (You et al., 2010).

The LOACs influence the NSWS showed a large uncertainty (Jiang et al., 2010; Fu et al., 2011). Former studies pointed out that the NAM could influence NSWS changes over China (Wu et al., 2018a; Shen et al., 2021; Zha et al., 2021b). However, possible processes of NAM impacts on the NSWS were not unraveled. Furthermore, changes in temperature gradient and pressure gradient are the driving force behind wind speed changes, and therefore, some studies suggested that the air temperature and pressure gradients play a predominant role to NSWS changes (You et al., 2010; Guo et al., 2011; Lin et al., 2013). The temperature/pressure gradient changes can be influenced by LOACs; however, how the LOACs influence the temperature/pressure gradient, and then NSWS, which are rarely analyzed over China. Consequently, in this study, we analyzed the possible processes of NAM affecting the NSWS in eastern China, and discuss the contributions of NAM to NSWS changes. The results provide a reference for improving our understanding of variations in LOACs that affect NSWS over China.

2. Datasets and methods

2.1. Datasets

The observed wind speed at 10 m (m s^{-1}) in 1979−2017 was obtained from China Meteorological Administration (CMA) (http://www.nmic.cn/site/index.html). The spatial pattern of total 587 stations in eastern China is presented in Fig. 1. Variables including the daily mean zonal wind (m s^{-1}), meridional wind (m s^{-1}), air temperature (K), sea-level pressure (Pa), and surface pressure (Pa), air temperature, and vertical velocity at 27 vertical levels from 1000 to 100 hPa in ERA5 are used. These variables have a spatial resolution of 0.75° × 0.75° over the Northern Hemisphere from 1979 to 2017 (Hersbach and Dee, 2016). Compared with the other global reanalysis products, the ERA5 reanalysis dataset exhibits better performance in describing the regional mean climate at a seasonal scale and representing the spatiotemporal variations of the wind speed (Ramon et al., 2019; Shen et al., 2022). The NAM index derived from Li and Wang (2003) is employed (http://lijianping.cn/dct/page/65571), which is a

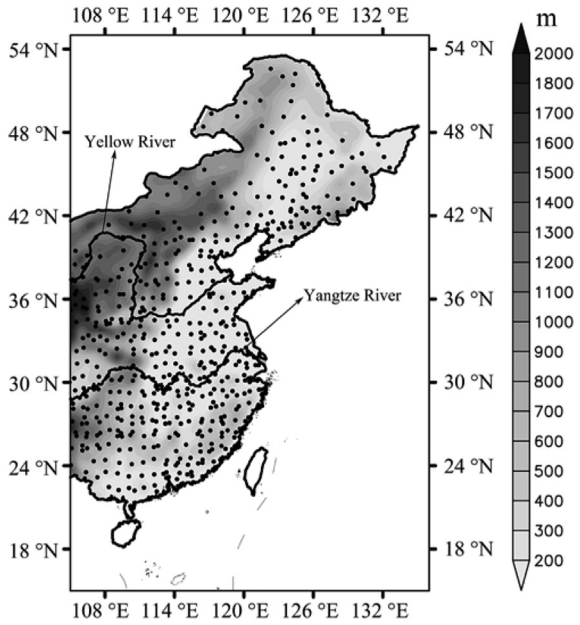

Fig. 1. Terrain height and meteorological stations over eastern China (Data were unavailable for Hainan and Taiwan provinces).

Please cite this article as: ZHA, J.-L et al., Effects of Northern Hemisphere Annular Mode on terrestrial near-surface wind speed over eastern China from 1979 to 2017, Advances in Climate Change Research, https://doi.org/10.1016/j.accre.2022.10.005

measure of the hemispheric-wide fluctuations in the surface air pressure occurring at the mid-to-high-latitude annular belt of actions. Compared to other zonal indices, the NAM index better reflects the zonal hemispheric change in the air mass, and therefore it has been extensively used to investigate the variations in atmospheric circulation (Baldwin and Thompson, 2009; Rotstaln et al., 2014).

2.2. Methods

Eastern China (15°−55°N, 105°−135°E) was selected as the study region owing to its dense meteorological stations and primarily flat topography. To ensure the confidence of wind speed data, the stations are selected based on the following criteria: 1) the station must be the national meteorological station; 2) there is no missing data in a whole year after 1979; 3) the total days of missing data account for less than 1% of the entire length; 4) the wind speed must be accompanied by the quality control code '0' in the datasets. We used the standard normal homogeneity test (SNHT) method (Alexandersson, 1986; Liu, 2000) to examine the homogenization of the chosen stations, which has been used extensively (Zhang et al., 2020; Shen et al., 2021). The SNHT is sensitive to the start and the end points of a sequence, such that a non-parametric *Pettitt*-test (Shen et al., 2021) is further employed to examine the stations that pass the SNHT. Based on the SNHT and the *Pettitt*-test, 587 stations passed the homogenization test and were thus selected (Fig. 1). To assess the consistency of the phases between two-time sequences, the probability of an anomaly appearing at the same time point in the two-time sequences is calculated (denoted by PAST) (Wu et al., 2018a; Zha et al., 2019a, 2019b).

The observed NSWS is decomposed into zonal and meridional components based on the wind direction of the ERA5 data, as the wind direction of the observational wind speed is not available. Correlation analysis and two-tailed Student's *t*-test are used to determine the significance of the data. The positive and negative values of the NAM index (NAMI) are defined as the positive NAM phase (NAM+) and negative NAM phase (NAM−), respectively. The Cressman objective analysis method is employed to interpolate the observational data to the grid at a resolution of 0.75° (Cressman, 1959). A Gaussian low-pass filter with a nine-year window is used to extract the decadal signals (Zhu et al., 2012), and the inter-annual sequence of the data is obtained based on the raw sequence subtracted the decadal sequence (Shen et al., 2022). The least-square method is used to calculate the linear trend.

3. Results

3.1. Spatiotemporal characteristics of NSWS

The NSWS decreased significantly from 1979 to 2017, at a rate of (−0.09 ± 0.01) m s^{-1} per decade ($p < 0.01$) for eastern China as a whole, with positive anomalies before 2000 and negative anomalies after that (Fig. 2a). A recovery of NSWS was also observed at a rate of (+0.21 ± 0.099) m s^{-1} per decade ($p < 0.10$) from 2010 to 2017. The zonal component (u) had a significant decreasing trend of (−0.04 ± 0.01) m s^{-1} per decade ($p < 0.01$), which accounted for 44.4% of the decreasing trend in the NSWS (Fig. 2b). The meridional component (v) also exhibited a decreasing trend, (−0.005 ± 0.014) m s^{-1} per decade ($p > 0.10$), which accounted for only 5.6% of the decreasing trend in NSWS (Fig. 2c). Furthermore, the correlation coefficients between the wind speed and the u and v values were 0.60 ($p < 0.01$) and 0.15 ($p > 0.10$), respectively. The PAST between the NSWS and the u value, and between the NSWS and the v value were 69.2 and 58.9%, respectively.

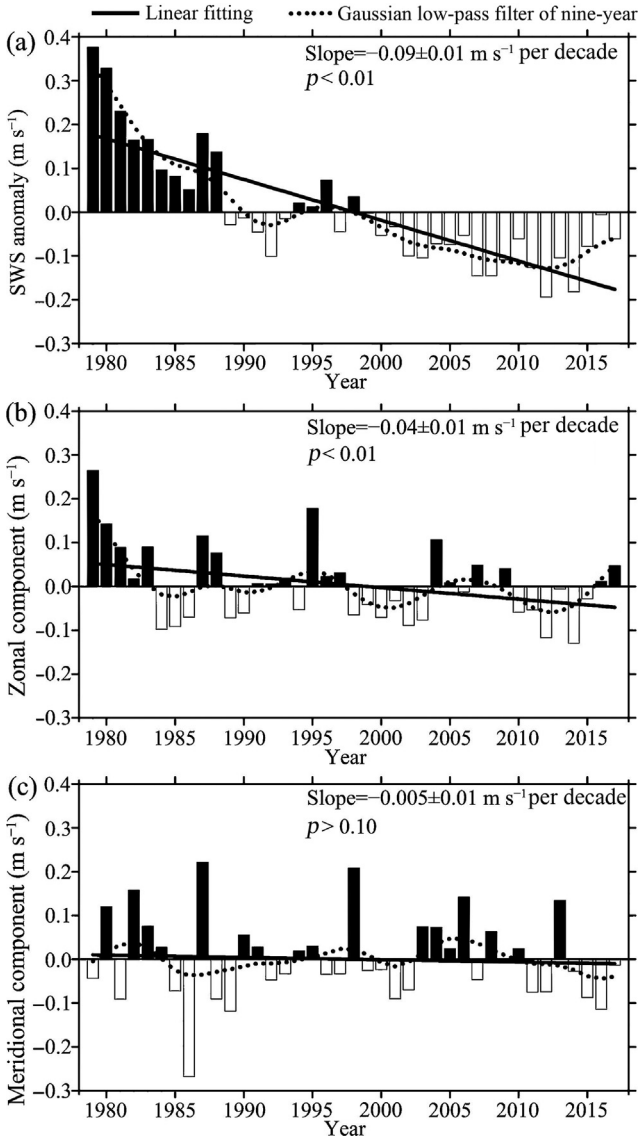

Fig. 2. Temporal changes of (a) NSWS anomaly, (b) zonal and (c) meridional component of observed NSWS during 1979−2017.

Spatial patterns of NSWS and the corresponding trends are shown in Fig. 3. The highest values exceeded 2.4 m s^{-1}, mainly in northeastern China, Inner Mongolia, the Shandong peninsula, and coastal regions (Fig. 3a). Significant ($p < 0.01$)

Please cite this article as: ZHA, J.-L et al., Effects of Northern Hemisphere Annular Mode on terrestrial near-surface wind speed over eastern China from 1979 to 2017, Advances in Climate Change Research, https://doi.org/10.1016/j.accre.2022.10.005

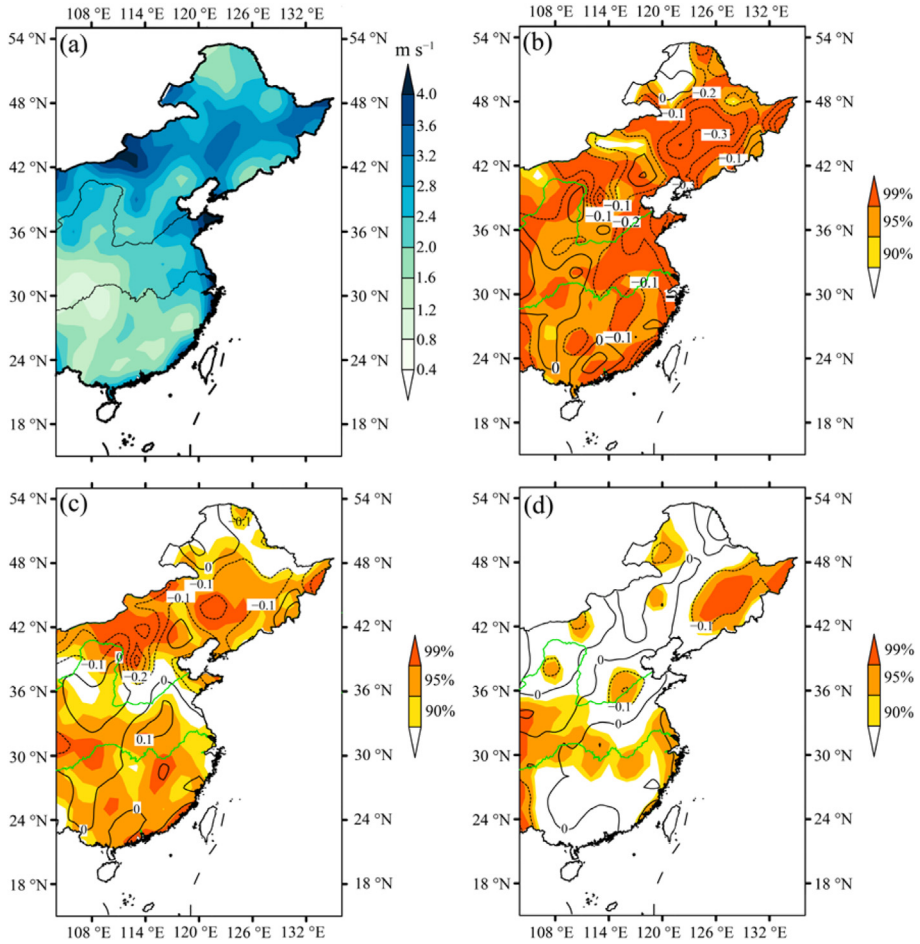

Fig. 3. Spatial patterns of (a) mean NSWS, linear trend of (b) NSWS, (c) zonal component, and (d) meridional component over eastern China during 1979−2017 (unit: m s^{-1} per decade) (Shades in (b−d) denote trends above the 90%, 95%, and 99% significant level, respectively).

decreasing trends are generally observed in northern parts of the Yellow River. The most substantial reduction in NSWS mainly occurs in northeastern China and some areas of the middle and lower reaches of the Yellow River and Yangtze River, this being −0.20 m s^{-1} per decade ($p < 0.01$). The slightest decrease in NSWS mainly occurs in central China, being less than −0.05 m s^{-1} per decade ($p < 0.10$) (Fig. 3b). A significant decreasing trend is also detected in u from 1979 to 2017, with trends exceeding −0.10 m s^{-1} per decade in northern China (Fig. 3c). A significant decreasing trend of v was only observed in the Yangtze River Valley and parts of northeastern China. Based on the results mentioned above, we concluded that the significant reduction in NSWS was mainly caused by the decrease in the u value.

3.2. Potential processes of NAM impacts on NSWS changes

Before revealing the impacts of NAM on NSWS changes over eastern China, the relationship between NAM and the large-scale wind field over the Northern Hemisphere is first analyzed. NAMI maintained strong positive phases, which were most substantial periods over the past 100 years (Li and Wang, 2003); NAM+ and NAM− accounted for 74.4% and 25.6% of 1979−2017, respectively (Fig. A1). During a NAM+, a negative wind speed anomaly occurred around 30°N, and a positive anomaly occurred around 60°N (Fig. 4a). The spatial pattern of the composite difference in u between NAM+ and NAM− (Fig. A2a) is consistent with Fig. 4a. The correlation coefficient between NAM and wind speed also exhibited a zonal pattern, with negative and positive correlation coefficients mainly located at mid- and high-latitudes, respectively (Fig. 4b). The spatial pattern of the correlation coefficient between the NAM and u value was also presented as a zonal annular belt (Fig. A2b). These results imply that the continuously warm phase of NAM is accompanied by the decrease in NSWS at the mid-latitudes of the Northern Hemisphere (China lies in this region), and the influence of the NAM on NSWS must be attributed to its modulation of zonal-mean westerlies.

Herein, we investigated the circulation behind the NAM that control the observed NSWS changes. Vertical attributes of

Please cite this article as: ZHA, J.-L et al., Effects of Northern Hemisphere Annular Mode on terrestrial near-surface wind speed over eastern China from 1979 to 2017, Advances in Climate Change Research, https://doi.org/10.1016/j.accre.2022.10.005

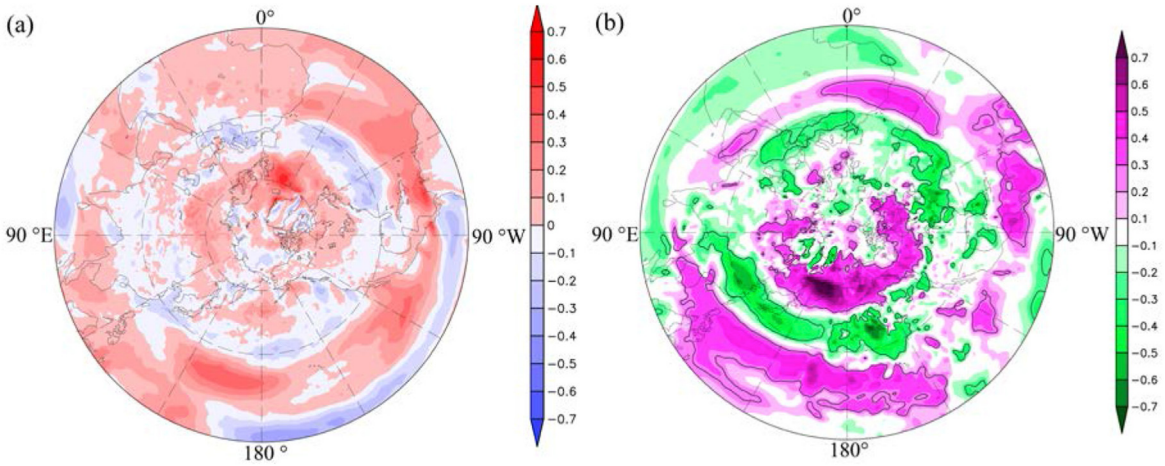

Fig. 4. Spatial patterns of composite difference in NSWS between positive and negative NAM phases (NAM + minus NAM−) (a), and correlation coefficients between NAM and NSWS over the Northern Hemisphere during 1979−2017 (b) (Contour in (b) represents the correlation coefficient exceeding the 90% confidence level).

the composite differences between NAM+ and NAM− are shown in Fig. 5. A negative zonal-mean u difference between NAM+ and NAM− was found at 10°−40°N, and a positive zonal-mean u difference was found from 40°N to polar (contour). Accordingly, accompanied by the NAM+, a strong westerly anomaly over the higher latitudes between 40°N and polar in the troposphere and a strong easterly anomaly over the subtropical latitudes between 10° and 40°N were observed, which are indicative of a weakened subtropical jet, a strengthened polar jet, and an enhancement in polar vortex strengths. A negative zonal-mean v difference between NAM+ and NAM− was found at 5°−35°N in the lower troposphere, and a positive zonal-mean v difference was located at 40°−65°N in the lower troposphere (shade). These results indicate that the southerly anomalies at 5°−35°N and the northerly anomalies at 40°−65°N in the lower troposphere are

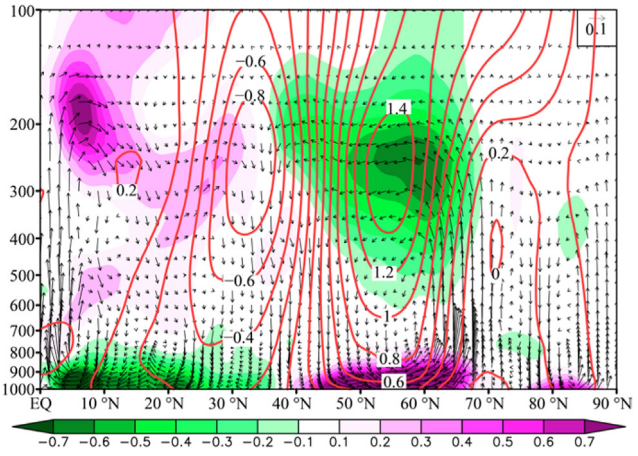

Fig. 5. Vertical structures of composite difference of zonal-mean v (shade), zonal-mean u (contour), and meridional circulation (vector) between NAM+ and NAM− (NAM+ minus NAM−) during 1979−2017 (The vector is that of the wind speed difference, whose two components are the zonal-mean v difference and the zonal-mean vertical velocity difference between NAM+ and NAM−).

accompanied by continuous NAM warm phases from 1979 to 2017. Anomalous ascending flows occurred at 60°−72°N, and anomalous descending flows occurred over mid-latitudes of 30°−50°N (vector). Hence, the Ferrell cell at high latitudes enhanced along with continuous NAM warm phases. Hence, NAM had considerable effects on the vertical circulations. These features were also presented during all four seasons (Fig. A3).

NAM caused the southerly anomalies in the lower troposphere over the mid-and high latitudes in the Northern Hemisphere. Meanwhile, the descending flows of the Ferrell cell further increased the southerly in the low troposphere. The increased southerly in the lower troposphere transported heat from middle latitudes to high latitudes near the surface, causing a rise in the surface air temperature (SAT) at mid-to-high latitudes. Consequently, the SAT was higher at mid-to-high latitudes of 30°−70°N during a NAM+ than those during a NAM− (Fig. 6a); a significant SAT difference occurred at mid-to-high latitudes of East Asia, which exceeded +0.8 °C ($p < 0.10$). The SAT at subtropical and low latitudes was lower during a NAM+ than those during a NAM−, although the SAT difference failed to pass the significance t-test at the 0.10 level. These results indicate that the SAT increases at mid-to-high latitudes can be associated with the continuous NAM warm phases from 1979 to 2017, especially in East Asia. The north−south SAT difference between mid-to-high latitudes and low latitudes over East Asia could decrease due to the significant positive SAT anomaly at mid-to-high latitudes in East Asia. Therefore, the north−south SAT difference between mid-to-high latitudes (35°−60°N, 60°−140°E) and low latitudes (0°−20°N, 60°−140°E) over East Asia (denoted as SATD) was estimated (Fig. 6b). SATD exhibited a downward trend of (−0.21 ± 0.07) °C per decade ($p < 0.01$). Meanwhile, NAM and SATD showed a negative correlation of −0.60 ($p < 0.01$) (Fig. 6c). These results indicate that NAM strengthening considerably reduced the SATD between mid-to-high latitudes and low latitudes of East Asia.

Please cite this article as: ZHA, J.-L et al., Effects of Northern Hemisphere Annular Mode on terrestrial near-surface wind speed over eastern China from 1979 to 2017, Advances in Climate Change Research, https://doi.org/10.1016/j.accre.2022.10.005

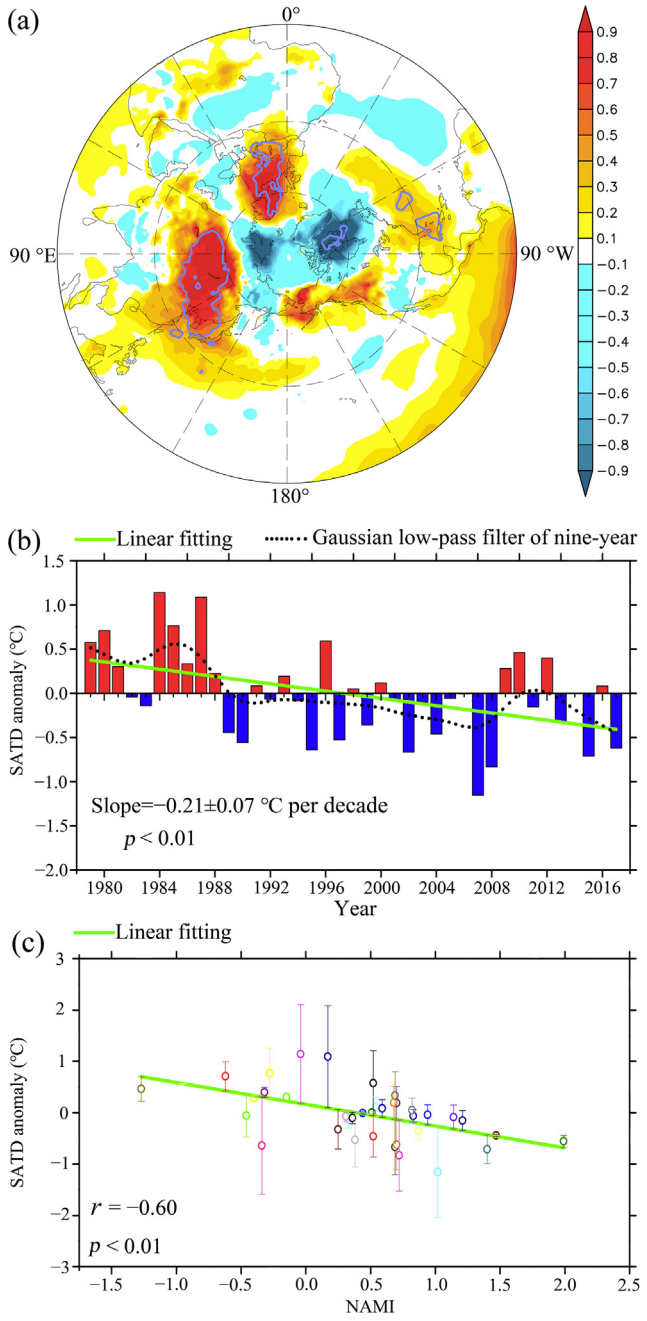

Fig. 6. Spatial pattern of the SATD between NAM+ and NAM− over Northern Hemisphere (NAM + minus NAM−) during 1979−2017 (a), (b) temporal changes of SATD between mid-to-high latitudes (35°−60°N, 60°−140°E) and low latitudes (0°−20°N, 60°−140°E) over East Asia during 1979−2017, and (c) regression analysis between SATD and NAM during 1979−2017. (The contours in (a) denote the SATD exceeding the 0.10 level. *r* in (c) denotes the correlation coefficient between NAMI and SATD, bars in (c) represent the chronic residual of the linear fitting, and different color dots in (c) represent different samples).

In Fig. 6a, a positive SAT difference was also observed east of 100°E. Thus, the west−east SAT variations could influence the temperature gradient. Consequently, the west−east gradient of SAT over two regions, 15°−50°N, 65°−105°E, and 15°−50°N, 105°−138°E, are analyzed (Fig. A4). The west−east SAT difference decreased from 1979 to 1998 at a rate of (−0.27 ± 0.08) °C per decade ($p < 0.01$), and increased from 1999 to 2017 at a rate of (+0.15 ± 0.08) °C per decade ($p < 0.10$). Compared to Fig. 6b, the temporal evolution of the west−east SAT difference was not consistent with those of the north−south SAT difference. Compared to Fig. 2a, the temporal evolution of the west−east SAT difference was also not consistent with those of the observed NSWS. Consequently, changes in the west−east SAT difference could not be the primary factor behind NSWS changes over eastern China.

According to the state equation $P = \rho RT$ (P is the pressure, ρ is the air density, R is air constant, and T is the air temperature), changes in SAT can influence pressure changes. Therefore, changes in north−south SATD can cause changes in the north−south pressure difference. Consequently, the pressure difference between mid-to-high latitudes (35°−60°N, 60°−140°E) and low latitudes (0°−20°N, 60°−140°E) is calculated (Fig. 7a). A downward trend in the surface pressure difference was observed at (−1.87 ± 0.69) Pa per year ($p < 0.01$). The pressure difference and SATD exhibits a significant correlation of +0.60 ($p < 0.01$) (Fig. 7b). Because the meridional pressure gradient affects the zonal wind, the relationship between the meridional pressure gradient and u value of the observed NSWS exhibits a positive correlation of +0.60 ($p < 0.01$) (Fig. 7c). In summary, the continuous NAM warm phase reduced the SATD, which weakened the meridional pressure gradient over East Asia and consequently, decreased NSWS in eastern China.

4. Discussion

4.1. Effects of NAM on the interannual variability of NSWS

A previous study indicates that the correlation between the NAM and the observed NSWS is more considerable at the interannual scale than those at the decadal scale (Wu et al., 2018a). Here, we investigated whether the physical processes behind the NAM-NSWS relationship can be better presented at the interannual scale and estimated the potential contribution of the NAM to interannual fluctuations of NSWS. To assess whether the freedom of the Gaussian low-pass filter influences the interannual variability of NSWS, the interannual sequence of NSWS is also extracted based on the raw series minus the linear fitting value. Results indicate that the interannual sequences of NSWS calculated based on two methods show consistent fluctuations (Fig. A5). Relationships between the NAM and the sea-level pressure (SLP) at different timescales were investigated. A significant positive (negative) correlation between NAMI and SLP was found at the belt of 30°N (60°N), which presents the typical NAM pattern (Fig. 8a and b). Compared to Fig. 4b, the annular belt pattern of the correlation coefficient between the NAM and zonal wind was efficiently reproduced at the interannual scale (Fig. 8c). The correlation between the NSWS over eastern China and the SLP field over the Northern Hemisphere likewise present the

Please cite this article as: ZHA, J.-L et al., Effects of Northern Hemisphere Annular Mode on terrestrial near-surface wind speed over eastern China from 1979 to 2017, Advances in Climate Change Research, https://doi.org/10.1016/j.accre.2022.10.005

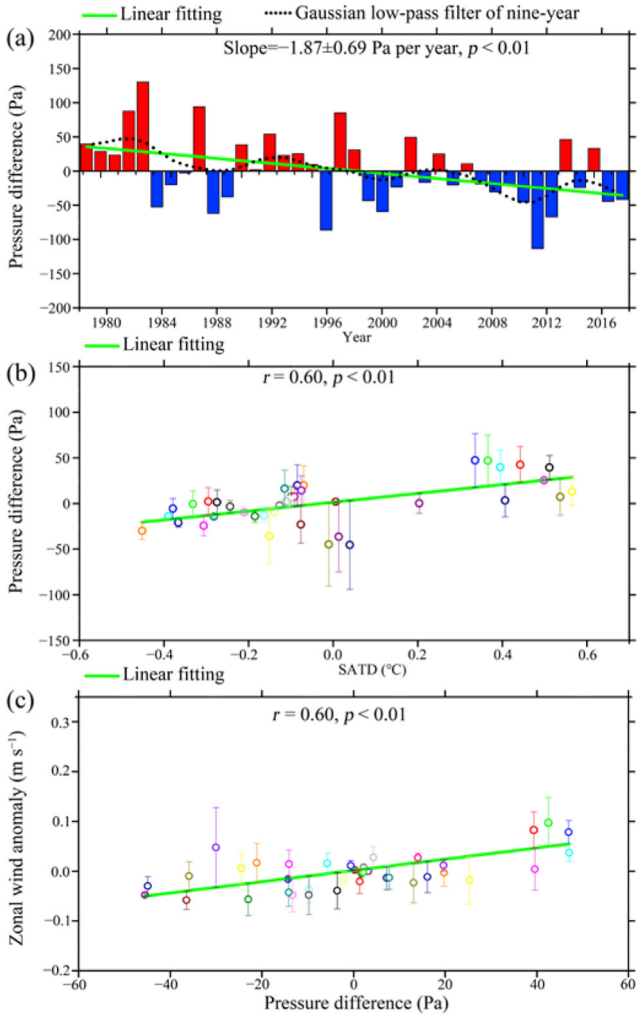

Fig. 7. (a) Temporal changes of north−south pressure difference (NSPD) anomaly between mid-to-high latitudes (35°−60°N, 60°−140°E) and low latitudes (0°−20°N, 60°−140°E) over East Asia for 1979−2017, and regression analysis between NSPD and SATD (u of observed NSWS) during 1979−2017 (b, c) (Bars in (b) and (c) represent the chronic residual of the linear fitting, and different color dots in (b) and (c) represent different samples).

typical NAM pattern at the interannual scale (Fig. 8d). However, a similar spatial pattern was not presented when decadal signals in the NSWS were included (Fig. 8e). Accordingly, the annular belt pattern of the correlation coefficient between the NSWS and the zonal wind was more remarkable at the interannual scale, especially around 30°N and 60°N. The quantified results are shown in Table A1. Furthermore, the effects of NAM on vertical circulations can be efficiently produced at the interannual scale, and the NSWS is also respond well to the changes in vertical circulation caused by the NAM at the interannual scale (Fig. A6). However, the vertical characteristics of the correlation coefficient between NSWS and zonal-mean v cannot be presented when the decadal signals of the NSWS are included. Detailed results are presented in Table A2.

To quantify the effects of NAM on the NSWS changes, we normalized the NAMI and NSWS and performed regression analyses at different timescales. The regression coefficients between NAMI and NSWS are considered as the relative contribution of the NAM to the NSWS changes. At the interannual scale, (32.0 ± 15.8)% of the observed annual mean NSWS over eastern China can be attributed to the NAM variations. The NAM contribution to the interannual variations of u over eastern China was more significant, reaching (45.0 ± 12.9)%. Nevertheless, the NAM contribution to the annual mean NSWS (u) over eastern China based on raw sequence was only (23.5 ± 15.2)% ((35.6 ± 13.1)%). Therefore, the NAM contribution to the zonal component in NSWS was more pronounced than those to the observed total wind speed at the same timescale.

4.2. Uncertainties

This study confirms that the NAM has a considerable effect on NSWS variations over eastern China, especially for the interannual changes in NSWS. However, there are several limitations and drawbacks. The wind direction of the observational daily mean NSWS is not available; therefore, the observed NSWS was decomposed into zonal and meridional components based on the wind direction of the ERA5 data. The ERA5 reanalysis dataset efficiently captures the interannual and monthly changes in NSWS, implying that the primary seasonal and interannual circulation features can be captured by the ERA5 reanalysis products (Shen et al., 2021b). Furthermore, we also used different reanalysis datasets to calculate the NAM index (e.g., ERA5, Hadley center, and NCAR sea-level pressures), and found that all NAM indices show consistent changes. Therefore, we considered that different reanalysis datasets used to calculate NAMI do not cause major discrepancies in the results. The long-term decrease in the SATD is associated with the continuous warm phase of NAM during the study period. If the NAM shows a strong alternation of cold and warm phases and exhibits increasing trends, such a change could cause an abnormal meridional circulation. However, it is unlikely to result in sustained warm air transport from low to high latitude and subsequently a sustained weakening of the north−south SATD. The potential effects of LOACs on the NSWS constitute a complex process (Zha et al., 2021b). Furthermore, it is a complicated process for NAM changes to affect temperature gradient and wind speed changes. The physical mechanisms of different LOACs affecting NSWS changes, and the physical and dynamical processes of how the NAM influences the NSWS by altering the temperature gradient must be further measured and investigated using numerical simulations based on a global climate model coupled with a regional climate model. These aspects are beyond the scope of this study, and should be addressed in the future.

Please cite this article as: ZHA, J.-L et al., Effects of Northern Hemisphere Annular Mode on terrestrial near-surface wind speed over eastern China from 1979 to 2017, Advances in Climate Change Research, https://doi.org/10.1016/j.accre.2022.10.005

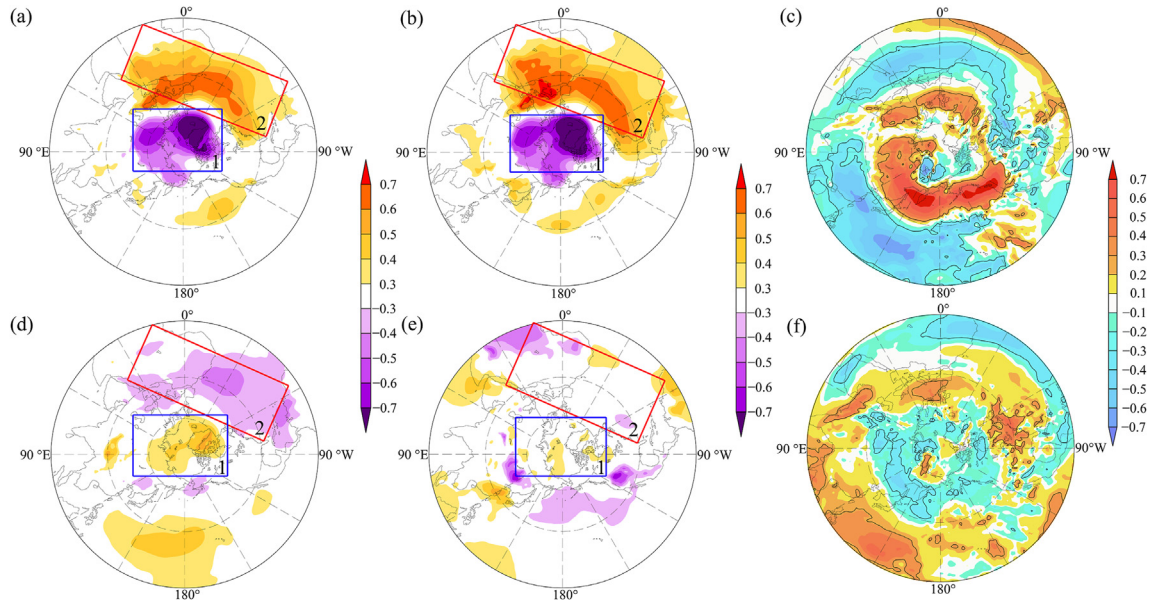

Fig. 8. Correlation coefficients between NAM and SLP (a, b), between NAM and *u* (c), between observed NSWS over eastern China and SLP (d, e), and between observed NSWS over eastern China and *u* (f) from 1979 to 2017. ((a), (c), (d), and f are calculated based on the interannual sequences; b and e are calculated based on the raw sequences. The contours in (c) and (f) denote the correlation coefficient of 0.27, which is the threshold for the 90% confidence level. Descriptions and analyses of boxes 1 and 2 are given in the Appendix).

5. Conclusions

This study reveals possible processes by which the NAM affects NSWS over eastern China. Results show that the decrease in the observed NSWS is dominated mainly by the weakening in the *u*. NAM has a considerable effect on NSWS changes in eastern China. During positive NAM phases, the zonal-mean westerly decreased over mid-latitudes, while the vertical movement was characterized by a descending flow at mid-latitudes (30°−50°N) and an ascending flow at 60°−72°N in the troposphere. The anomalous meridional flows transported heat from lower latitudes to higher latitudes, thereby reducing the meridional SATD, which further decreased the driving force of NSWS over eastern China and caused NSWS changes. NAM could generate a stronger effect on interannual changes in NSWS than the interdecadal changes in NSWS. Furthermore, at the interannual scale, NAM could have a more noticeable influence on the *u* value than the total wind speed. Quantitatively, (32.0 ± 15.8)% of the observed annual mean NSWS over eastern China can be attributed to NAM variations. In contrast, the NAM contribution to the interannual variations in *u* of the observed NSWS could reach (45.0 ± 12.9)%.

Declaration of competing interest

The authors declare no conflict of interest.

Acknowledgments

The authors cordially thank the anonymous reviewers and editors for their thorough comments and constructive suggestions, which greatly improve the quality of this study. The work was supported by the National Key Research and Development Program of China (2018YFA0606004), Natural Science Foundation of China (42005023, 41875178, 41865001), Swedish Formas (2019-00509 and 2017-01408), and VR (2021-02163 and 2019-03954). This work is also supported by the High-level Talents Program of Yunnan University, the Program for "Xingdian" Talent of Yunnan Province, the Program for Key Laboratory at the University of Yunnan Province, and the Chinese Jiangsu Collaborative Innovation Center for Climate Change.

Appendix A. Supplementary data

Supplementary data to this article can be found online at https://doi.org/10.1016/j.accre.2022.10.005.

References

Alexandersson, H., 1986. A homogeneity test applied precipitation data. Int. J. Climatol. 6, 661−675.
Azorin-Molina, C., Vicente−Serrano, S.M., McVicar, T.R., et al., 2014. Homogenization and assessment of observed near-surface wind speed trends over Spain and Portugal, 1961−2011. J. Clim. 27, 3692−3712.
Baldwin, M.P., Thompson, D.W.J., 2009. A critical comparison of stratosphere-troposphere coupling indices. Q. J. R. Meteorol. Soc. 135, 1661−1672.
Chen, L., Li, D., Pryor, S.C., 2013. Wind speed trends over China: quantifying the magnitude and assessing causality. Int. J. Climatol. 33, 2579−2590.
Cressman, G.P., 1959. An operational objective analysis system. Mon. Weather Rev. 87, 367−374.
Dadaser-Celik, F., Cengiz, E., 2014. Wind speed trends over Turkey from 1975 to 2006. Int. J. Climatol. 34, 1913−1927.
Earl, N., Dorling, S., Hewston, R., et al., 2013. 1980−2010 variability in U.K. surface wind climate. J. Clim. 26, 172−1191.
Fu, G.B., Yu, J.J., Zhang, Y.C., et al., 2011. Temporal variation of wind speed in China for 1961−2007. Theor. Appl. Climatol. 104, 313−324.

Guo, H., Xu, M., Hu, Q., 2011. Changes in near-surface wind speed in China: 1969–2005. Int. J. Climatol. 31, 349–358.
Guo, X.Y., Wang, L., Tian, L.D., et al., 2017. Elevation-dependent reductions in wind speed over and around the Tibetan Plateau. Int. J. Climatol. 37, 1117–1126.
Hersbach, H., Dee, D., 2016. ERA5 reanalysis is in production. ECMWF Newsletter No 147, 7.
Jerez, S., Trigo, R.M., Vicente–Serrano, S.M., et al., 2013. The impact of the North Atlantic Oscillation on the renewable energy resources in south-western Europe. J. Appl. Meteorol. Climatol. 52, 2204–2225.
Jiang, Y., Luo, Y., Zhao, Z.C., et al., 2010. Changes in wind speed over China during 1956–2004. Theor. Appl. Climatol. 99, 421–430.
Kim, Z.B., Paik, K., 2015. Recent recovery of surface wind speed after decadal decrease: a focus on South Korea. Clim. Dynam. 45, 1699–1712.
Laapas, M., Venalainen, A., 2018. Homogenization and trend analysis of monthly mean and maximum wind speed time series in Finland, 1959–2015. Int. J. Climatol. 37, 4803–4813.
Li, J.P., Wang, J.X.L., 2003. A modified zonal index and its physical sense. Geophys. Res. Lett. 30, 1632.
Li, X., Li, Q.P., Ding, Y.H., et al., 2021. Near-surface wind speed changes in eastern China during 1970–2019 winter and its possible causes. Adv. Clim. Change Res. 13, 228–239.
Li, Y., Chen, Y., Li, Z., et al., 2018. Recent recovery of surface wind speed in Northwest China. Int. J. Climatol. 38, 4445–4458.
Lin, C.G., Yang, K., Qin, J., et al., 2013. Observation coherent trends of surface and upper-air wind speed over China since 1960. J. Clim. 26, 2891–2903.
Liu, X.N., 2000. The homogeneity test on mean annual wind speed over China. Quart. J. Appl. Meteorol. 11, 28–34 (Chinese).
Malloy, J.W., Krahenbuhl, D.S., Bush, C.E., et al., 2015. A surface wind extremes ("Wind Lulls" and "Wind Blows") climatology for central North America and adjoining oceans (1979–2012). J. Appl. Meteorol. Climatol. 54, 643–657.
McVicar, T.R., van Niel, T.G., Li, L.T., et al., 2007. Spatial distributing monthly reference evapotranspiration and pan evaporation considering topographic influences. J. Hydrol. 338, 196–220.
McVicar, T.R., Roderick, M.L., Donohue, R.J., et al., 2012. Global review and synthesis of trends in observed terrestrial near-surface wind speeds: implications for evaporation. J. Hydrol. 416, 182–205.
Pryor, S.C., Barthelmie, R.J., 2011. Assessing climate change impacts on the near-term stability of the wind energy resource over the United States. Proc. Natl. Acad. Sci. U. S. A 108, 8167–8171.
Ramon, J., Lledó, L., Torralba, V., et al., 2019. What global reanalysis best represents near-surface winds? Q. J. R. Meteorol. Soc. 145, 3236–3251.
Roderick, M.L., Rotstayn, L.D., Farquhar, G.D., et al., 2007. On the attribution of changing pan evaporation. Geophys. Res. Lett. 34, 251–270.
Rotstaln, L.D., Plymin, E.L., Collier, M.A., et al., 2014. Declining aerosols in CMIP5 projections: effects on atmospheric temperature structure and midlatitude Jets. J. Clim. 27, 6960–6967.
Shen, C., Zha, J.L., Wu, J., et al., 2021. Centennial-scale variability of terrestrial near-surface wind speed over China from reanalysis. J. Clim. 34, 5829–5846.
Shen, C., Zha, J.L., Wu, J., et al., 2022. Does CRA-40 outperform other reanalysis products in evaluating near-surface wind speed changes over China. Atmos. Res. 266, 1–12.
Shi, P., Zhang, G., Kong, F., et al., 2019. Variability of winter haze over the Beijing–Tianjin–Hebei region tied to wind speed in the lower troposphere and particulate sources. Atmos. Res. 215, 1–11.
Tobin, I., Jerez, S., Vautard, R., et al., 2016. Climate change impacts on the power generation potential of a European mid-century wind farms scenario. Environ. Res. Lett. 11, 034013.
Vautard, R., Cattiaux, J.H., Yiou, P., et al., 2010. Northern Hemisphere atmospheric stilling partly attributed to an increase in surface roughness. Nat. Geosci. 3, 756–761.
Wan, H., Wang, X., Swail, V.R., 2010. Homogenization and trend analysis of Canadian near-surface wind speeds. J. Clim. 23, 1209–1225.
Wu, J., Zha, J., Zhao, D., 2016. Estimating the impact of the changes in land use and cover on the surface wind speed over the East China Plain during the period 1980–2011. Clim. Dynam. 46, 847–863.
Wu, J., Zha, J., Zhao, D., 2017. Evaluating the effects of land use and cover change on the decrease of surface wind speed over China in recent 30 years using a statistical downscaling method. Clim. Dynam. 48, 131–149.
Wu, J., Zha, J., Zhao, D., et al., 2018a. Changes of wind speed at different heights over Eastern China during 1980–2011. Int. J. Climatol. 38, 4476–4495.
Wu, J., Zha, J., Zhao, D., et al., 2018b. Changes in terrestrial near-surface wind speed and their possible causes: an overview. Clim. Dynam. 51, 2039–2078.
Wu, J., Han, Z.Y., Yan, Y.P., et al., 2021. Future changes in wind energy potential over China using RegCM4 under RCP emission scenarios. Adv. Clim. Change Res. 12, 596–610.
Xu, M., Chang, C.P., Fu, C., et al., 2006. Steady decline of East Asian monsoon winds, 1969–2000: evidence from direct ground measurements of wind speed. J. Geophys. Res. Atmos. 111, D24111.
Yang, X.M., Li, Z.X., Feng, Q., et al., 2012. The decreasing wind speed in southwestern China during 1969–2009, and possible causes. Quat. Int. 263, 71–84.
You, Q., Kang, S., Flugel, W.A., et al., 2010. Decreasing wind speed and weakening latitudinal surface pressure gradients in the Tibetan Plateau. Clim. Res. 42, 57–64.
Zeng, Z., Ziegler, A.D., Searchinger, T., et al., 2019. A reversal in global terrestrial stilling and its implications for wind energy production. Nat. Clim. Change 9, 979–985.
Zha, J., Wu, J., Zhao, D., 2017a. Effects of land use and cover change on the near-surface wind speed over China in the last 30 years. Prog. Phys. Geogr. Earth Environ. 41, 46–67.
Zha, J., Wu, J., Zhao, D., et al., 2017b. Changes of the probabilities in different ranges of near-surface wind speed in China during the period for 1970–2011. J. Wind Eng. Ind. Aerod. 169, 156–167.
Zha, J., Wu, J., Zhao, D., et al., 2019a. A possible recovery of the near-surface wind speed in Eastern China during winter after 2000 and the potential causes. Theor. Appl. Climatol. 136, 119–134.
Zha, J., Zhao, D., Wu, J., et al., 2019b. Numerical simulation of the effects of land use and cover change on the near-surface wind speed over Eastern China. Clim. Dynam. 53, 1783–1803.
Zha, J., Zhao, D., Wu, J., et al., 2021a. Terrestrial near-surface wind speed variations in China: research and prospects. J. Meteorol. Res. 35, 537–556.
Zha, J., Shen, C., Zhao, D., et al., 2021b. Slowdown and reversal of terrestrial near-surface wind speed and its future changes over eastern China. Environ. Res. Lett. 16, 034028.
Zha, J., Shen, C., Li, Z., et al., 2021c. Projected changes in global terrestrial near-surface wind speed in 1.5°C–4.0°C global warming levels. Environ. Res. Lett. 16, 114016.
Zhang, G., Azorin-Molina, C., Shi, P., et al., 2019a. Impact of near-surface wind speed variability on wind erosion in the eastern agro-pastoral transitional zone of Northern China, 1982-2016. Agric. For. Meteorol. 271, 102–115.
Zhang, R., Zhang, S., Luo, J., et al., 2019b. Analysis of near-surface wind speed changes in China during 1958–2015. Theor. Appl. Climatol. 137, 2785–2801.
Zhang, G., Azorin-Molina, C., Chen, D., et al., 2020. Variability of daily maximum wind speed across China, 1975–2016: an examination of likely causes. J. Clim. 33, 2793–2816.
Zhang, Z., Wang, K., 2020. Stilling and recovery of the surface wind speed based on observation, reanalysis, and geostrophic wind theory over China from 1960 to 2017. J. Clim. 33, 3989–4008.
Zhao, D., Zha, J., Wu, J., 2020. Changes in daily cumulative volumetric rainfall at various intensity levels due to urban surface expansion over China. Tellus A Dynam. Meteorol. Oceanogr. 72, 1–21.
Zhao, D., Zha, J., Wu, J., 2021. Changes in rainfall of different intensities due to urbanization-induced land-use changes in Shenzhen, China. Clim. Dynam. 56, 2509–2530.
Zhu, J., Liao, H., Li, J., 2012. Increases in aerosol concentrations over eastern China due to the decadal-scale weakening of the East Asian summer monsoon. Geophys. Res. Lett. 39, L09809.

Please cite this article as: ZHA, J.-L et al., Effects of Northern Hemisphere Annular Mode on terrestrial near-surface wind speed over eastern China from 1979 to 2017, Advances in Climate Change Research, https://doi.org/10.1016/j.accre.2022.10.005